Desalination and Water Treatment
www.deswater.com

10 (2009) 134–138

1944-3994 / 1944-3986

An approach to theoretical prediction of permeate flux decline in ultrafiltration

María-Cinta Vincent-Vela[a], Enrique Bergantiños-Rodríguez[b], Silvia Álvarez-Blanco[a]*, Jaime Lora-García[a]

[a]*Department of Chemical and Nuclear Engineering, Polytechnic University of Valencia, C/Camino de Vera s/n 46022 Valencia, Spain Tel. +34 963877000 Ext. 76383; Fax +34 963877639; email: sialvare@iqn.upv.es*
[b]*Department of Chemical Engineering, Polytechnical Institute José A. Echeverría, Ave. 114, No. 11901, Havana, Cuba*

Received 22 July 2008; Accepted in revised form 2 September 2009

ABSTRACT

Permeate flux decline was predicted by means of Song and Elimelech's [1] model. Theoretical results were compared with those obtained in ultrafiltration experiments where TMP and crossflow velocity were varied. Polyethylene glycol (PEG) of 35000 Da was used in the feed solution in a concentration of 10 g/L. The experiments were performed with monotubular ultrafiltration ceramic (Al_2O_3–TiO_2) membranes of 5 kDa (Tami Industries, France). The model predicted a reduction in the influence of transmembrane pressure (TMP) on permeate flux as TMP increased. This was consistent with the experimental results for the lowest crossflow velocity tested (1 m/s). For higher crossflow velocities the reduction in the influence of TMP on permeate flux as TMP increased was higher than that predicted by the model. Model predictions were better for low crossflow velocities, as expected with a model that considers cake formation as the main fouling mechanism. Rapid initial pore blocking may be the main cause of the discrepancies observed between experimental results and theoretical predictions.

Keywords: Permeate flux decline; Ultrafiltration; Polyethylene glycol; Pore blocking; Cake formation

1. Introduction

Membrane technology is being widely applied in many industrial processes concerning biotechnology, pharmacy, food, drinking water production, wastewater treatment, etc. [2]. However, fouling is a barrier for membrane technology application. Membrane fouling reduces permeate flux production and can result in a non viability for application. This phenomenon is related to the non-steady character of membrane microfiltration and ultrafiltration processes [3]. Therefore, steady-state models that attempt to describe ultrafiltration processes are not appropriate for this purpose.

Many researchers have tried to develop a generalized model capable of adequately describing microfiltration and ultrafiltration processes. Despite the advances attained, there is not an available model that suits the expectations. Some models are empirical or semi-empirical models and they require experimentation prior to modelling.

A theoretical dynamic model that precisely describes an ultrafiltration process can provide the same information that can be experimentally obtained. Moreover, it facilitates the understanding of the physical and/or chemical phenomena involved in the separation process and it offers a powerful tool for prediction, control, computer simulation and optimization of industrial processes, etc.

Recent advances in the theoretical description of dynamic models focused on: application of dead-end filtration models for crossflow ultrafiltration [4], cake formation mechamisms [1,5,6], combined cake formation

* Corresponding author.

Presented at EuroMed 2008, Desalination for Clean Water and Energy Cooperation among Mediterranean Countries of Europe and the MENA Region, 9–13 November 2008, King Hussein Bin Talal Convention Center, Dead Sea, Jordan.

and pore blocking models [7], etc. These models were analyzed and modified in many occasions [8–19]

This work focuses on Song and Elimelech's [1] dynamic model, which is one of the most integral and versatile models. It also provides information about the restrictions in the applicability of the model when macromolecular solutes are used and analyses the connection between model hypothesis, experimental results and model predictions. Overall, this work represents a tool for seeking an ultrafiltration dynamic model capable of accurately simulating the process for a wide range of operational conditions.

2. Modelling

Song and Elimelech [1] developed a model that considered three important concepts in ultrafiltration: concentration polarisation, gel layer formation and critical pressure. Critical pressure, ΔP_{cc}, is directly related to concentration polarisation, gel layer formation and fouling. Critical pressure can be defined as the pressure above which gel layer begins to form. Therefore, according to the model, two layers co-exist: the gel layer directly formed over the membrane surface and the concentration polarisation layer formed above the gel layer. Other approaches can be also found in the literature. For example Bhattacharjee and Datta considered the boundary layer problem and the gel layer formation simultaneously with the film theory of mass transfer and resistance in series model [19]. According to the model proposed by Song and Elimelech, below critical pressure, only the concentration polarisation layer exists. In this case, this layer is directly formed over the membrane surface and not over the gel layer. If the gel layer concentration is represented by the symbol C_g, the concentration polarisation layer can only achieve a maximum concentration value just below, C_g. The critical pressure can be calculated from the critical filtration number [1], N_{FC}, by means of Eq. (1):

$$N_F = \frac{4\pi \ a_p^3}{3kT} \ \Delta P_c \tag{1}$$

where N_F is the filtration number, a_p is the particle or molecular radius, k is the Boltzman's constant; T is the temperature and ΔP_c is the pressure loss in the concentration polarisation layer. When ΔP_c takes the value of ΔP_{cc}, then N_F takes the value of N_{FC}.

The critical filtration number can be estimated from the gel layer concentration in (v/v), C_{GV}, by means of Eq. (2) [9]:

$$N_{FC} = \int_0^{\theta_{GV}} \frac{1+\frac{2}{3}\theta^5}{1-\frac{3}{2}\theta+\frac{3}{2}\theta^5-\theta^6} \ 3\theta^2 \ d\theta \tag{2}$$

In Eq. (2) $\theta = C_V^{1/3}$ and C_v is concentration (v/v).

The model developed by Song and Elimelech [1] considered that steady-state was achieved when the thickness of the gel layer remained constant all over the membrane surface. Under non-steady state conditions two separated regions exist over the membrane surface: the equilibrium region and the non-equilibrium region. The equilibrium region is characterised by an instant formation of the gel layer, meaning a rapid achievement of steady-state. This region is located near the feed solution inlet. The non-equilibrium region corresponds to the rest of the membrane surface, where steady-state is slowly reached.

The permeate flux over the whole membrane, $J_m(t)$, can be calculated as follows [1]:

$$J_m(t) = \frac{1.31}{L}\left[\frac{C_g D^2 \gamma}{C_o} x(t)^2\right]^{1/3} + \frac{L-x(t)}{L} J(t) \tag{3}$$

where L is the membrane length, D is the diffusion coefficient of the solute, C_g and C_o are the concentration in the gel layer and in the feed, respectively, γ is the shear rate, $x(t)$ is the frontier location between the equilibrium region and the non-equilibrium region, $J(t)$ is the permeate flux in the non-equilibrium region and t is time. Model parameters $x(t)$ and $J(t)$ can be calculated as follows:

The frontier location, $x(t)$, is given by Eq. (4) [1]:

$$x(t) = 4.81\left(D^2\gamma\right)\left(\frac{C_o}{C_g}\right)^{1/2}\left(\frac{r_c}{\Delta P - \Delta P_{cc}} t\right)^{3/2} \tag{4}$$

where ΔP is the transmembrane pressure and r_c is the intrinsic resistance of the gel layer.

Finally, the permeate flux in the non-equilibrium region, $J(t)$, is given by Eq. (5) [1]:

$$J(t) = \frac{\left(\Delta P - \Delta P_c\right)}{\mu R_m}\left[1 + \frac{2r_c\left(\Delta P - \Delta P_c\right)}{\mu^2 R_m^2}\frac{C_o}{C_g} t\right]^{-1/2} \tag{5}$$

The parameters included in Eq. (5) can be estimated from the following equations:

According to Carman–Kozeny equation [Eq. (6)] for the flow across a porous media, the specific resistance of the cake layer can be calculated as follows [4,8,20]:

$$r_c = \frac{45\mu(1-\varepsilon)^2}{a_p^2 \varepsilon^3} \tag{6}$$

where μ is the dynamic viscosity of the permeate, $\varepsilon = (1 - C_{GV})$ is the cake layer porosity and a_p is the radius of the solute molecule.

The Stokes–Einstein radius of PEG is related to its molecular weight (MW) by Eq. (7) [21]. All the variables in Eq. (7) are expressed in the international system of units (SI). Eq. (7) is valid for a MW range of 200–40000 g/mol and has been very often used [22,23].

$$a_p = \left(0.262 \cdot (\mathrm{MW})^{0.5} - 0.3\right) \cdot 10^{-10} \quad (7)$$

The diffusivity of PEG at 25°C can be correlated with the MW of the molecule by means of Eq. (8) [2,24]. Other correlations for the diffusivity of PEG as a function of the MW can be found in the literature [25–27], but they were found to be less accurate.

$$D = 9.82 \cdot 10^{-9} \cdot (\mathrm{MW})^{-0.52} \quad (8)$$

The shear rate at the membrane surface is given by Eq. (9) [4,12,28].

$$\gamma = \frac{4 \cdot v_{\mathrm{tang}} \cdot \left[\pi \cdot \left(\frac{D_{\mathrm{int}}}{2}\right)^2\right]}{\pi \cdot D_{\mathrm{int}}^3} \quad (9)$$

where v_{tang} is the crossflow velocity and D_{int} is the internal diameter of the membrane.

For tubular membranes and turbulent flow the gel layer concentration is estimated by means of Eq. (10) [29].

$$\frac{C_g}{C_0} = \exp\left(\frac{J_m \cdot D_{\mathrm{int}}{}^{0.11} \cdot \upsilon^{0.56}}{0.023 \cdot v_{\mathrm{tang}}{}^{0.89} \cdot D^{0.67}}\right) \quad (10)$$

where υ is the kinematic viscosity of the permeate.

The calculation sequence used in the simulation of permeate flux was the following: First, the mean radius of PEG molecules, solute diffusivity and shear rate were estimated according to Eqs. (7)–(9). After that, the gel concentration estimated by means of Eq. (10) was used in Eq. (6) to calculate the specific resistance of the gel layer. The critical filtration number was estimated using Eq. (2) and it was used to estimate the critical pressure by means of Eq. (1). Afterwards, the frontier location and the permeate flux in the non equilibrium region as a function of time were obtained [Eqs. (4), (5)] and substituted in Eq. (3) to finally obtain a function of time that describes the permeate flux over the whole membrane.

3. Materials and methods

Monotubular TiO_2/Al_2O_3 ceramic membranes with a molecular weight cut-off (MWCO) of 5 kg/mol from Tami Industries (France) were selected for the ultrafiltration experiments. The membrane area was 35.25 cm^2. The experiments were carried out at a constant temperature (25°C) and a constant feed concentration (10 g/L of polyethylene glycol (PEG) of 35 kg/mol). Transmembrane pressure (TMP) and crossflow velocity were varied in the interval of 0.2–0.5 MPa and 1–3 m/s for TMP and crossflow velocity, respectively.

Membrane cleaning was performed at 40°C with a 0.25 g/L NaOCl solution (pH was adjusted at 11 by NaOH addition). As the cleaning protocol was optimum, the same membrane was used in all the experiments. Permeate flux was fully recovered after the cleaning process.

Ultrafiltration tests were performed with the ultrafiltration pilot plant described elsewhere [13,14,16]. Fig. 1 shows a schematic diagram of the plant. The relative error committed in the determination of the permeate flux was calculated according to previous works [13], resulting in a relative error equal or lower than 11.

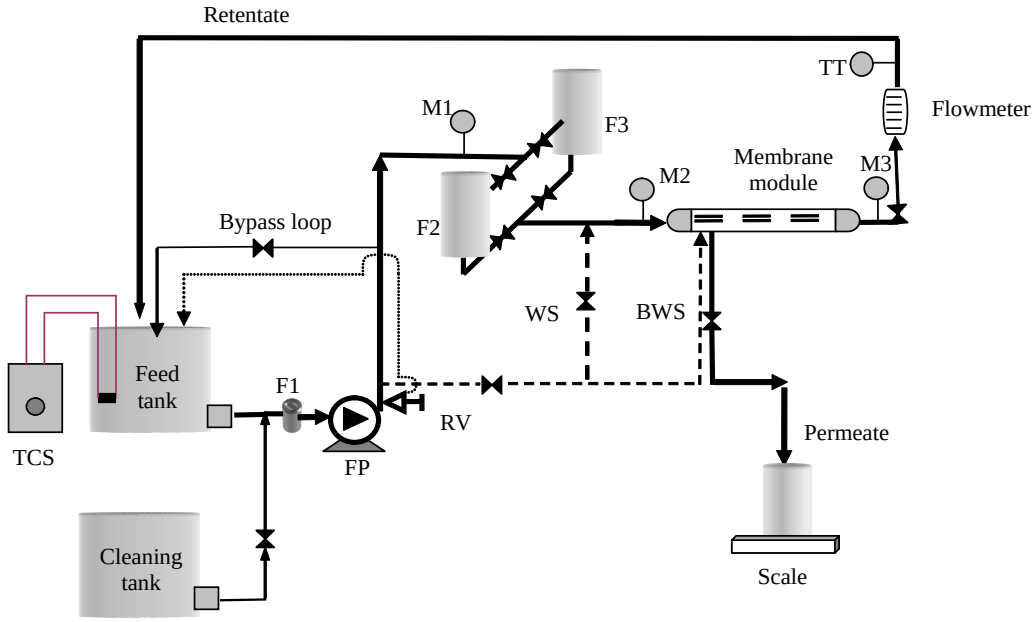

Fig. 1. Diagram of the ultrafiltration pilot plant used in the experiments. F: Filter; FP: Feed pump; M: Manometer; RV: Security valve; WS: washing system; BWS backwashing system; TCS: temperature control system; TT: temperature transducer.

4. Results and discussion

Experimental and predicted permeate flux decline are compared in Figs. 2–4. Fig. 2 represents the results obtained for a crossflow velocity of 1 m/s. Rapid initial pore blocking may be the main cause of the discrepancies observed between experimental results and theoretical predictions for short time scales. Initial pore blocking may occur at the beginning of the ultrafiltration experiments. Nevertheless, this phenomenon occurs so fast that it could not be detected in the experimental results. The best concordance between experimental and predicted results occurs at the lowest TMP tested (2 MPa). For this TMP the model predicts the lowest permeate flux decline. However, the model predicts a steady-state permeate flux inferior to that experimentally observed for all the TMPs tested. Moreover, steady-state permeate flux is achieved later for model predictions than observed for the experimental data, except for a TMP of 2 MPa.

The results obtained for a crossflow velocity of 2 m/s (Fig. 3) are worse than those obtained for a crossflow velocity of 1 m/s because the probability of gel layer formation is lower for high crossflow velocities. The best results are again obtained for the lowest TMP tested. For low TMPs, initial pore blocking may not be as relevant as for high TMP.

For the highest crossflow velocity tested (Fig. 4), differences between experimental and predicted initial permeate flux are the smallest. Due to high crossflow velocities, initial fouling diminishes. Consequently, the pore blocking fouling of the membrane, which causes a rapid initial flux decline, is reduced. The experimental results obtained for the lowest TMP are the nearest to the model predictions. It can also be observed comparing Figs. 2–4 for the experimental results, that as crossflow velocity increases, TMP has a greater effect on permeate flux values.

The time needed to achieve steady-state predicted by the model increases as TMP augments. Moreover, the difference between the initial permeate flux experimentally obtained and the one predicted by the model noticeably increases with TMP. The explanation for this could be that, for short time scales, a fouling mechanism (instantaneous adsorption of molecules and/or pore blocking) not considered by the model is occurring. This is in accordance with the fact that the best results are obtained for low TMP. Pore blocking is more severe for high TMPs.

It must also be noted that the discrepancies between experimental and predicted results may be due to several additional facts. The model analysed in this paper does not consider solute-solute interactions which are considered in other models [30]. Moreover, it makes some approximations to obtain an analytical solution (concentration polarization layer very thin compared to the channel height, membrane resistance neglected when concentration polarization is appreciably developed, immobile gel layer, fluid field in the channel undisturbed by the gel layer) which may also contribute to these discrepancies [31].

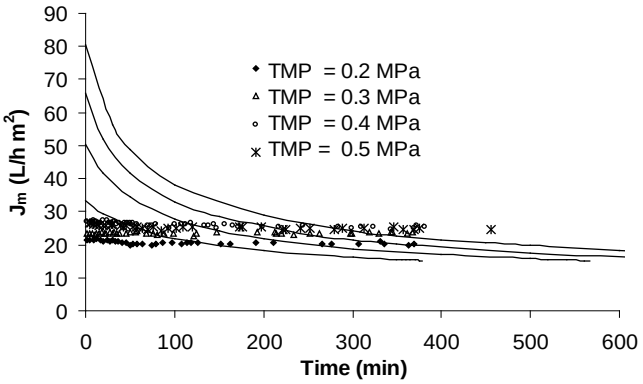

Fig. 2. Experimental data and model predictions for a crossflow velocity of 1 m/s.

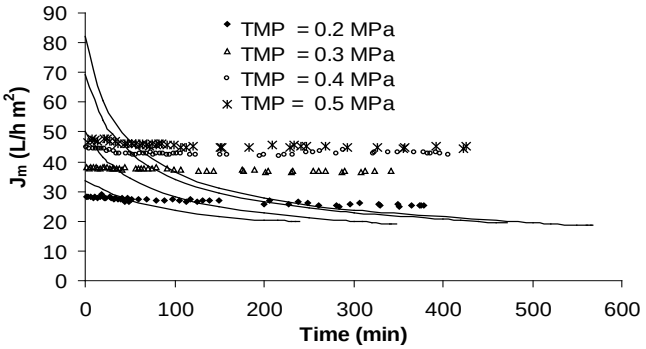

Fig. 3. Experimental data and model predictions for a crossflow velocity of 2 m/s.

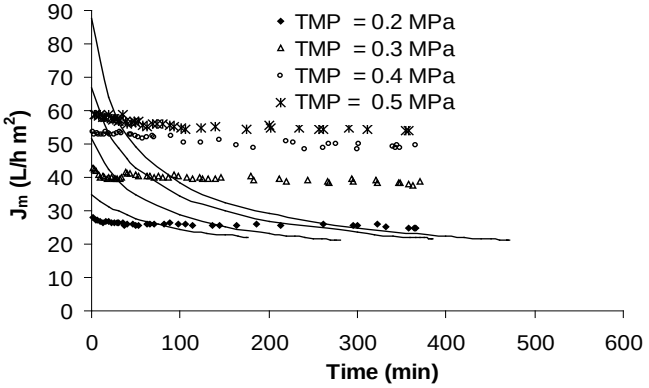

Fig. 4. Experimental data and model predictions for a crossflow velocity of 3 m/s.

5. Conclusions

Model predictions were better for low crossflow velocities, as expected with a model that considers cake formation as the main fouling mechanism. Moreover, model predictions for changes in permeate flux with crossflow velocity are lower than in the case of experimental results. The large differences between predicted and experimental initial permeate flux decline together with the best model predictions obtained for low TMPs, suggests that a fouling mechanism is taking place for short time scales that it is not considered by the model. This phenomenon may be occurring preferably at the highest TMPs set in the experiments.

Acknowledgements

The authors of this work wish to gratefully acknowledge the financial support of the Spanish Ministry of Science and Technology (MCYT) through its project no. CTQ2005-03398.

References

[1] L. Song and M. Elimelech, Theory of concentration polarization in cross-flow filtration. J. Chem. Soc., Faraday Trans., 91 (1995) 3389–3398.
[2] M. Cheryan, Ultrafiltration and Microfiltration Handbook. 2nd ed., CRC Press, New York, 1998.
[3] M. Mulder, Basic Principles of Membrane Technology. 2nd ed., Kluwer Academic, Dordrecht, 2000.
[4] R.H. Davis, Modeling of fouling of crossflow microfiltration membranes, Separ. Purif. Meth., 21 (1992) 75–126.
[5] P.K. Bhattacharya and S. Bhattacharjee, Flux decline behaviour with low molecular weight solutes during ultrafiltration in an unstirred batch cell. J. Membr. Sci., 72 (1992) 149–161.
[6] N. Mugnier, J.A Howell and M. Ruf, Optimisation of a back-flush sequence for zeolite microfiltration, J. Membr. Sci., 175 (2000) 149–161.
[7] C.C. Ho and A.L. Zydney, A combined pore blockage and cake filtration model for protein fouling during microfiltration. J. Coll. Interf. Sci., 232 (2000) 389–399.
[8] L. Song, Flux decline in cross-flow microfiltration and ultrafiltration: mechanisms and modelling of membrane fouling. J. Membr. Sci., 139 (1998) 183–200.
[9] L. Song, A new model for the calculation of the limiting flux in ultrafiltration. J. Membr. Sci., 144 (1998) 173–185.
[10] L. Wang and L. Song, Flux decline in cross-flow microfiltration and ultrafiltration: experimental verification of fouling dynamics. J. Membr. Sci., 160 (1999) 41–45.
[11] M. Zhang and L. Song, Mechanisms and parameters affecting flux decline in cross-flow microfiltration and untrafiltration of colloids. Env. Sci. Tech., 34 (2000) 3767–3773.
[12] M. Zhang and L. Song, Pressure-dependent permeate flux in ultra and microfiltration, J. Env. Eng., 126 (2000) 667–674.
[13] M.C. Vincent-Vela, S. Álvarez-Blanco and J. Lora-García, Cross-flow ultrafiltration of cake forming solutes: a non-steady state model. Desalination, 184 (2005) 347–356.
[14] M.C. Vincent-Vela, S. Álvarez-Blanco, J. Lora-García and E. Bergantiños-Rodríguez, Prediction of flux decline in the ultrafiltration of macromolecules. Desalination, 192 (2006) 323–329.
[15] M.C. Vincent-Vela, S. Álvarez-Blanco, J. Lora-García and E. Bergantiños-Rodríguez, Application of a dynamic model that combines pore blocking and cake formation in crossflow ultrafiltration. Desalination, 200 (2006) 138–139.
[16] M.C. Vincent-Vela, S. Álvarez-Blanco, J. Lora-García and E. Bergantiños-Rodríguez, Application of a dynamic model for predicting flux decline in crossflow ultrafiltration. Desalination, 198 (2006) 303–309.
[17] M.C. Vincent-Vela, S. Álvarez-Blanco, J. Lora-García, J.M. Gozálvez-Zafrilla and E. Bergantiños-Rodríguez, Modelling of flux decline in crossflow ultrafiltration of macromolecules: comparison between predicted and experimental results. Desalination, 204 (2007) 328–334.
[18] M.C. Vincent-Vela, S. Álvarez-Blanco, J. Lora-García, J.M. Gozálvez-Zafrilla and E. Bergantiños-Rodríguez, Utilization of a shear induced diffusion model to predict permeate flux in the crossflow ultrafiltration of macromolecules. Desalination, 206 (2007) 61–68.
[19] C. Bhattacharjee and S. Datta, Numerical simulation of continuous stirred ultrafiltration process: An approach based on moving boundary layer concept, Sep. Sci. Tech., 38 (2003) 1749–1772.
[20] G. Belfort, R.H. Davis and A.L. Zydney, The behaviour of suspensions and macromolecular solutions in crossflow ultrafiltration, J. Membr. Sci., 96 (1994) 1–58.
[21] C Tam and A. Tremblay, Membrane pore characterization — comparison between single and multicomponent solute probe techniques, J. Membr. Sci., 57 (1991) 271–287.
[22] P. Puhlfürβ, A. Voigt, R. Weber and M. Morbe, Microporous TiO_2 membranes with a cut off < 500 Da, J. Membr. Sci., 174 (2000) 123–133.
[23] D. Möckel, E. Staude and M.D. Guiver, Static protein adsorption, ultrafiltration behaviour and cleanability of hydrophilized polysulfone membranes, J. Membr. Sci., 158 (1999) 63–75.
[24] P. Prádanos, J.I. Arribas and A. Hernández, Mass transfer coefficient and retention of PEGs in low pressure cross-flow ultrafiltration through asymmetric membranes, J. Membr. Sci., 99 (1995) 1–20.
[25] C. Bhattacharjee and S. Datta, Analysis of mass transfer during ultrafiltration of PEG-6000 in a continuous stirred cell: effect of back transport, J. Membr. Sci., 119 (1996) 39–46.
[26] S. Das Gupta and P.K. Bhattacharya, Comparative limiting flux analysis of black liquor and polyethylene glycol in ultrafiltration, Chem. Eng. Comm., 93 (1990) 193–210.
[27] T.K. Sherwood, R.L. Pigford and C.R. Wilke, eds., Mass Transfer, McGraw Hill, New York, 1975.
[28] R.C. Castro, H.G. Monbouquette and Y. Cohen, Shear-induced permeability changes in a polymer grafted silica membrane, J. Membr. Sci., 179 (2000) 207–220.
[29] S. Lee, J. Kim and C.H. Lee, Analysis of $CaSO_4$ scale formation mechanism in various nanofiltration modules, J. Membr. Sci., 163 (1999) 63–74.
[30] S. Bhattacharjee, A.S. Kim and M. Elimelech, Concentration polarization of interacting solute particles in crossflow membrane filtration, J. Coll. Interf. Sci., 212 (1999) 81–99.
[31] M. Elimelech and S. Bhattacharjee, A novel approach for modeling concentration polarization in crossflow membrane filtration based on the equivalence of osmotic pressure model and filtration theory, J. Membr. Sci., 145 (1998) 223–241.